

NORSAR

ROYAL NORWEGIAN COUNCIL FOR SCIENTIFIC AND INDUSTRIAL RESEARCH

NORSAR Scientific Report No. 1-86/87

SEMIANNUAL TECHNICAL SUMMARY

1 April - 30 September 1986

L.B. Loughran (ed.)

Kjeller, November 1986



APPROVED FOR PUBLIC RELEASE, DISTRIBUTION UNLIMITED

VII.2 On three-component analysis of secondary phases

In a previous report we discussed the relative performance of arrays and three-component stations in the analysis of regional P phases (Kværna and Doornbos, 1986). An important aspect of this analysis is the determination of a covariance matrix $\underline{\underline{C}}$ of the form

$$C_{nm}(\underline{s}) = \int F_n(\omega, \underline{s}) F_m^*(\omega, \underline{s}) d\omega/2\pi \quad (1)$$

where the signals have been phase shifted for slowness \underline{s} :

$$F_n(\omega, \underline{s}) = F_n(\omega) \exp(i\omega \underline{s} \cdot \underline{x}_n)$$

and $F_n(\omega)$ is the Fourier spectrum at channel n . Using $\underline{\underline{C}}$ of eq. (1), the generalization of conventional beamforming is given by the normalized response

$$P(\underline{s}) = \underline{g}^+ \underline{\underline{C}} \underline{g} / \{ |\underline{g}|^2 \text{tr } \underline{\underline{C}} \} \quad (2)$$

where \underline{g} is the predicted displacement vector for slowness \underline{s} . The generalization of optimum beamforming methods proceeds similarly, but eq. (2) is sufficient for our present purpose.

Eq. (2) involves no explicit assumption about the phase type, and so may be applicable in the analysis of secondary phases as well. The success of such an analysis depends on our ability to predict the vector \underline{g} in eq. (2). Put another way, it depends on the ability to match the covariance matrix $\underline{\underline{C}}$, since

$$\underline{g}^+ \underline{\underline{C}} \underline{g} = \text{tr}(\underline{\underline{C}} \underline{\underline{G}}) , \quad \underline{\underline{G}} = \underline{g} \underline{g}^+$$

In this regard we note the following points: (1) The particle displacement of S is relatively complicated even in simple models. The fact that in its simplest form, plane wave S motion is polarized in a plane implies that from the observed direction of S motion at a given time one cannot uniquely infer the slowness vector; the solution vec-

tors span the plane perpendicular to the direction of S motion. Only when the SV/SH ratio is known can a unique solution be obtained. This is not usually the case. The problem is aggravated when interaction with the surface and near-surface structure is taken into account (see below). (2) For a single component array of sensors, the \underline{g} vector in eq. (2) is constant and the operation (2) is trivial. For a three-component sensor, \underline{g} represents the predicted displacement vector for slowness \underline{s} . The prediction is model-dependent. For example, \underline{g} will be frequency independent if a uniform half-space model is used to account for surface interaction. In the real earth this is usually not the case, not even for P waves. Fig. VII.2.1 shows the results of an analysis of three-component records from the broadband station in NORESS. The records give the P wave from an event in the Hindu Kush (Fig. VII.2.1a). The slowness solutions, in the form of apparent velocity and azimuth (Fig. VII.2.1b), show significant dispersion violating the assumption of frequency independent \underline{g} . The correct values are near the SP solution for apparent velocity, and near the LP solution for azimuth. This suggests that relatively small-scale lateral structure is the dominant source of azimuth bias, whereas the apparent velocity for P is mostly affected by large-scale vertical structure. Indeed, a simple modification of the uniform half-space model by introducing a discontinuity between the upper and lower crust at 15 km depth, does produce velocity dispersion of the observed order of magnitude (Fig. VII.2.2). The calculations in this and other one-dimensional models are based on a stripped version of Kennett's (1983) reflectivity algorithm. (The required modifications were made by Kennett during a visit to NORSAR this summer.) Of course, this and other models introduced here are not meant to have any significance other than that they give an indication of the required scale of inhomogeneity.

For short-period S there is little difference between the response of the two-layer crustal model and that of a uniform half space (as is the case for short-period P). The uniform half-space response for SV gives a ratio of horizontal to vertical displacement, for slowness p :

$$u_h/u_v = (1/\beta^2 - 2p^2)/(2p/1/\alpha^2 - p^2) \quad (3)$$

where α and β are the P and S velocity, respectively.

The SV particle motion for the uniform half-space model is plotted in Fig. VII.2.3. Note that the regional S_n phase has an apparent velocity of about 4.5-5.0 km/s, hence $p \approx 0.20-0.22$ s/km, and the predicted motion is elliptical with the long axis vertical. However, the observed response is quite different. Fig. VII.2.4 displays the 3 components of a typical regional S_n phase. The response is dominated by horizontal motion. The particle motion of S_n from three different events is plotted in Fig. VII.2.5, showing almost rectilinear SV motion with the long axis horizontal.

It is well known that S interacts strongly with crustal inhomogeneity, and three-dimensional models are certainly required to account for the observed effects. However, even simple modifications of a one-dimensional model can produce dramatic effects. Fig. VII.2.6 displays the SV particle motion when adding a thin (200 m) low-velocity layer on top of the crust. The effect of the layer is to change the long axis of SV motion from vertical to horizontal for a wide range of slowness encompassing the slowness of S_n . The modification does not affect the P motion. It is emphasized again that the model has no significance other than to indicate the required scale of inhomogeneities. The result suggests that 3-component data of regional S are unsuitable for slowness analysis. At best one can infer the azimuth

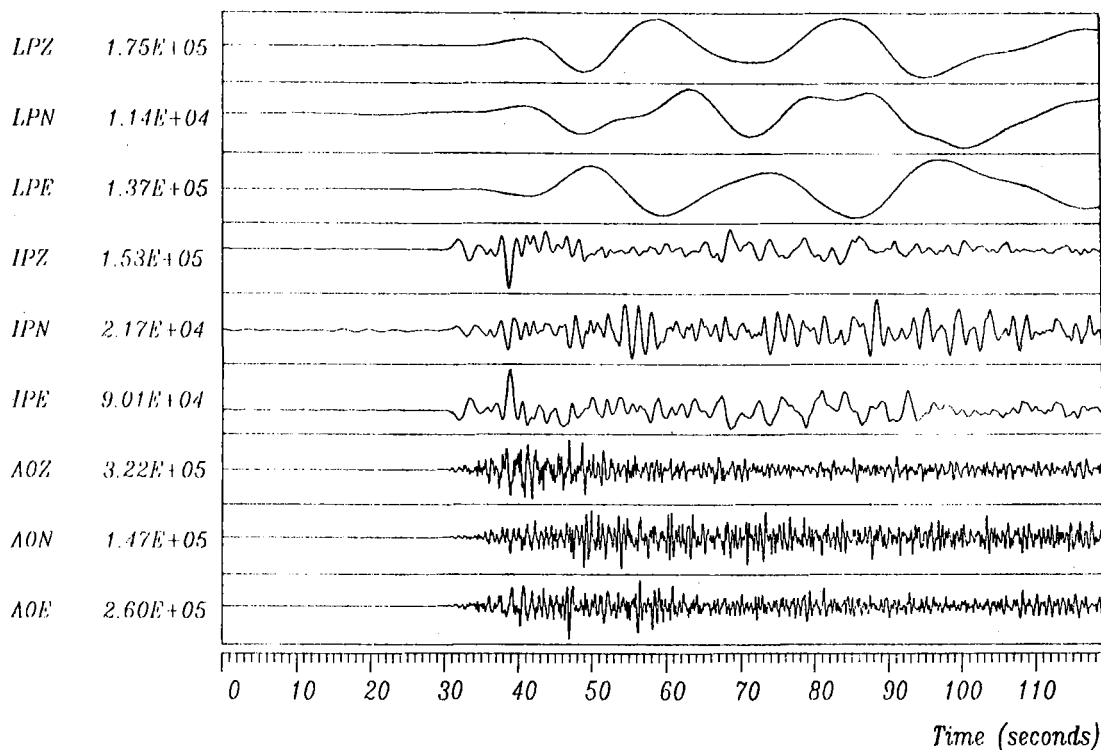
apart from a 180° ambiguity, and only if the SV/SH ratio is known. On the other hand, due to the response characteristics should horizontal components have potential for detection of S_n .

T. Kværna
D.J. Doornbos

References

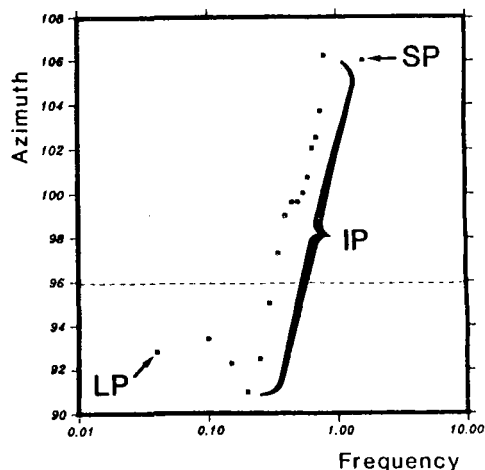
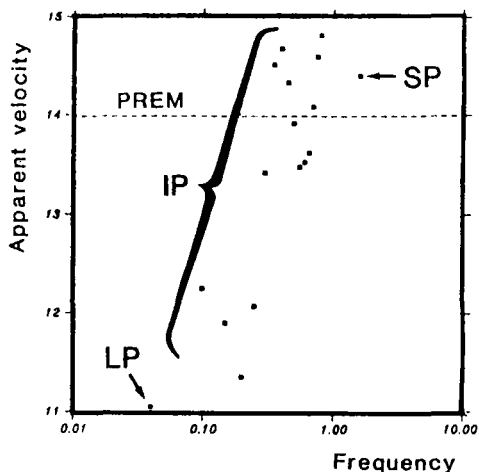
- Kennett, B.L.N. (1983): Seismic Wave Propagation in Stratified Media, 342 pp. Cambridge Univ. Press.
- Kværna, T. and D.J. Doornbos (1986): An integrated approach to slowness analysis with arrays and three-component stations. Semiann. Tech. Summary, 1 Oct 85 - 32 Mar 86, NORSAR Sci. Rep. No. 2-85/86.

HINDU KUSH MB 6.6 DEPTH 99 KM



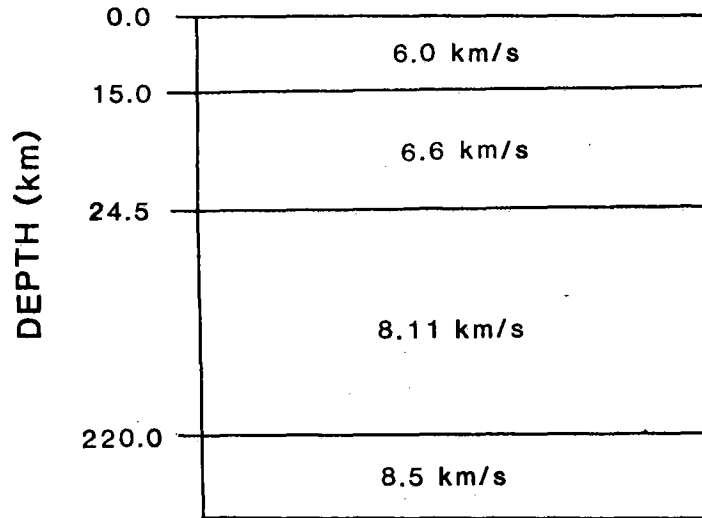
a)

Hindu Kush mb 6.6 depth 99 km



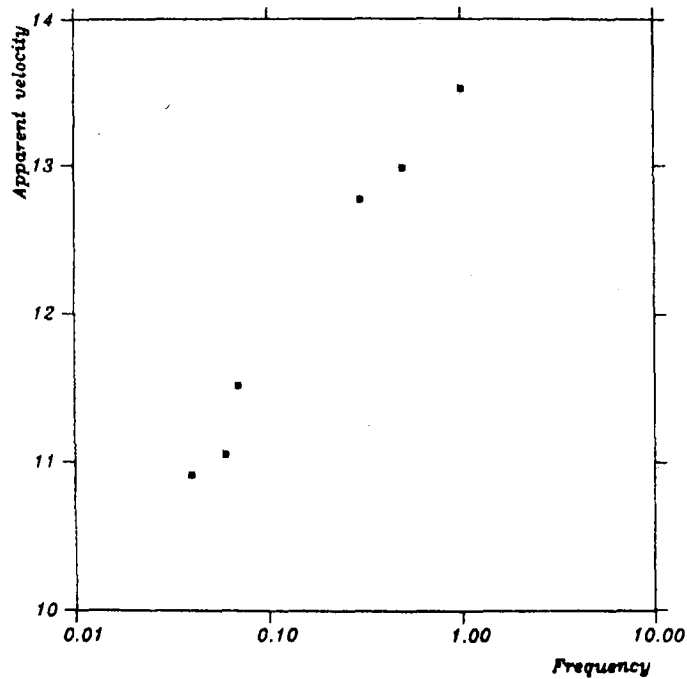
b)

Fig. VII.2.1 a) P wave from event in Hindu Kush recorded in three different frequency bands of the broadband station in NORESS.
 b) Slowness solutions as a function of frequency, using uniform half space model with $v_p = 6.0$ km/s, $v_s = 3.46$ km/s. Slowness vector decomposed in apparent velocity and azimuth.



a)

Synthetic PREM model data



b)

Fig. VII.2.2 a) Crustal model used to generate synthetic broadband P.
b) Slowness solutions when applying the uniform half-space model ($v_p = 60$ km/s, $v_s = 3.46$ km/s) to the synthetic data generated in model in a).

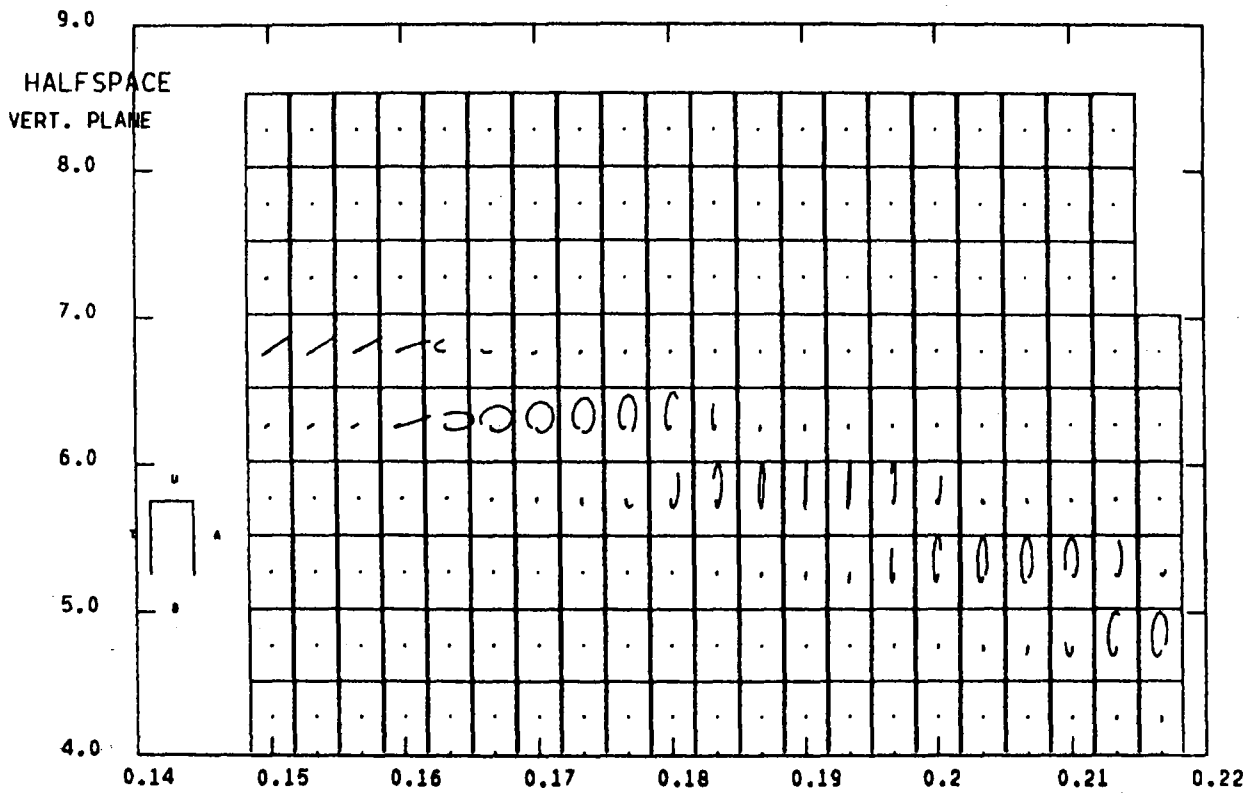


Fig. VII.2.3 Particle displacement as a function of slowness and time. Synthetic data represent the response of the uniform half space to incident plane SV wave.

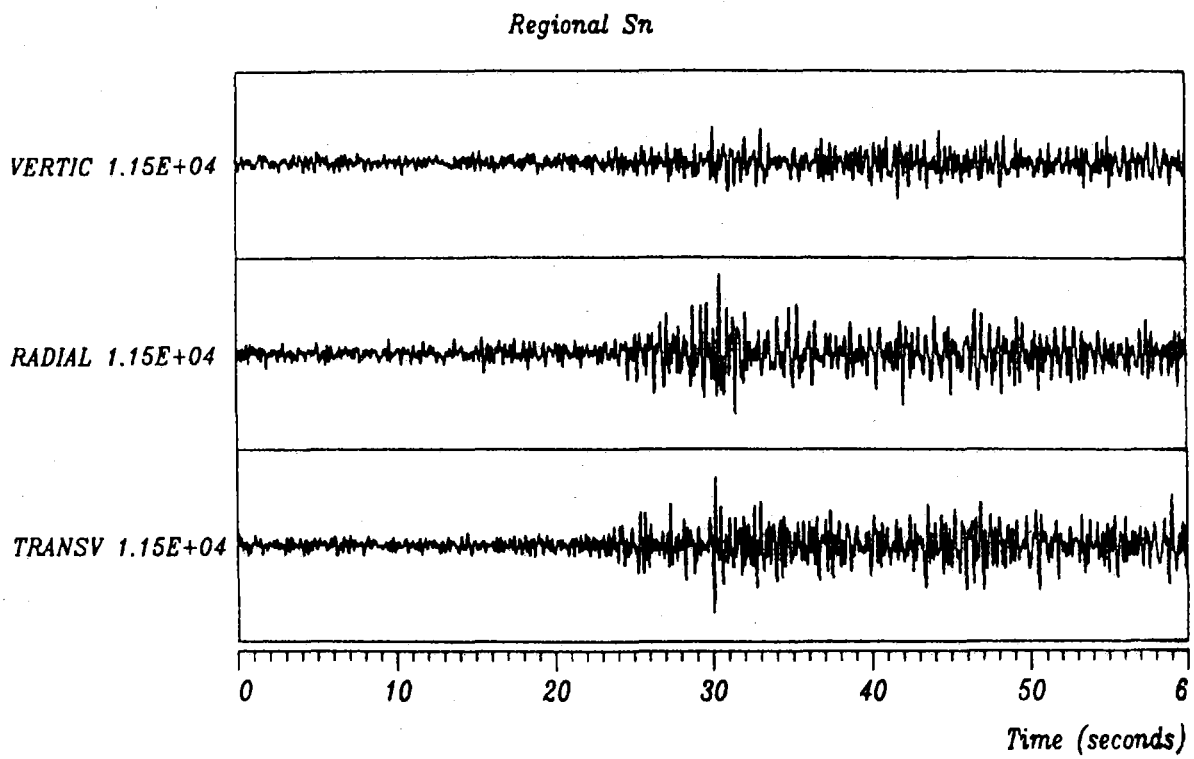


Fig. VII.2.4 Typical three-component seismograms of regional S_n . All traces are scaled to the same value.

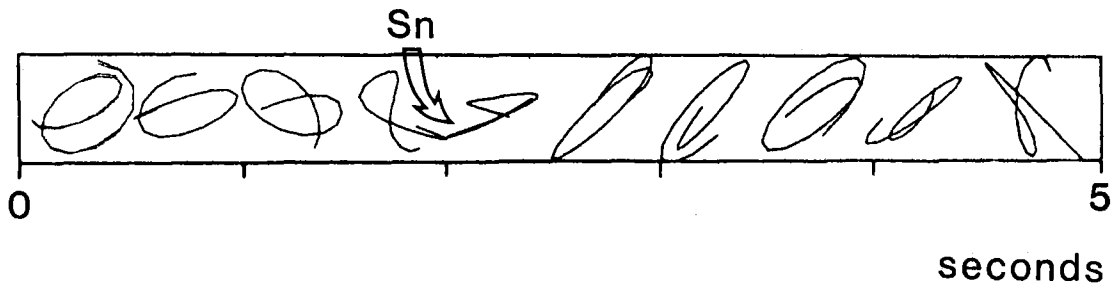
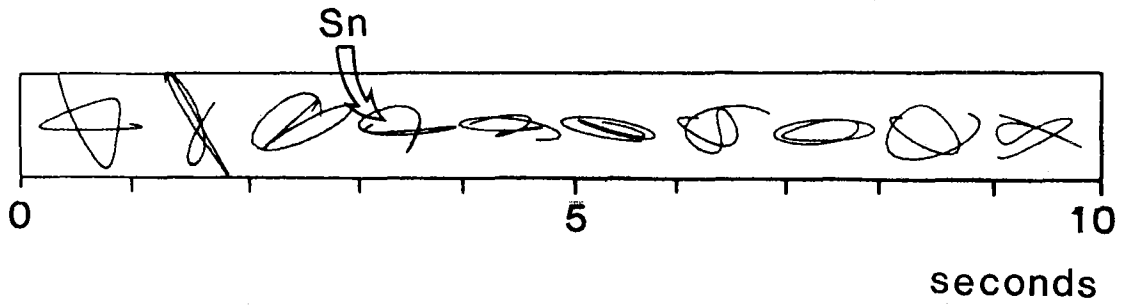
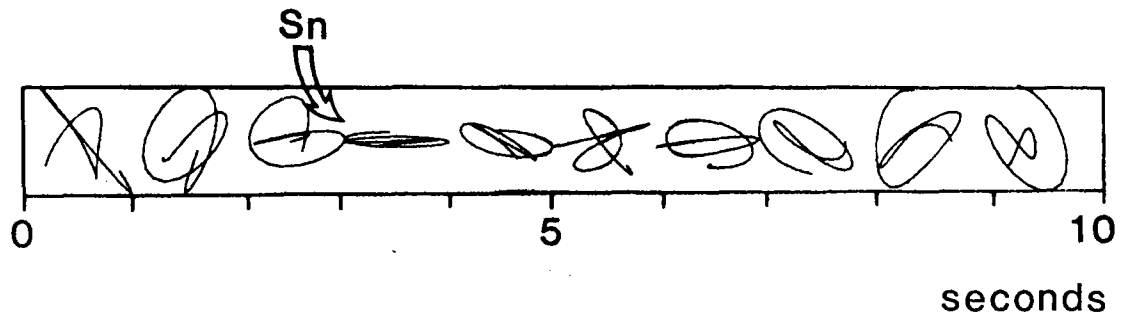


Fig. VII.2.5 Particle motion in the vertical-radial plane of SV, for S_n from three different regional events.

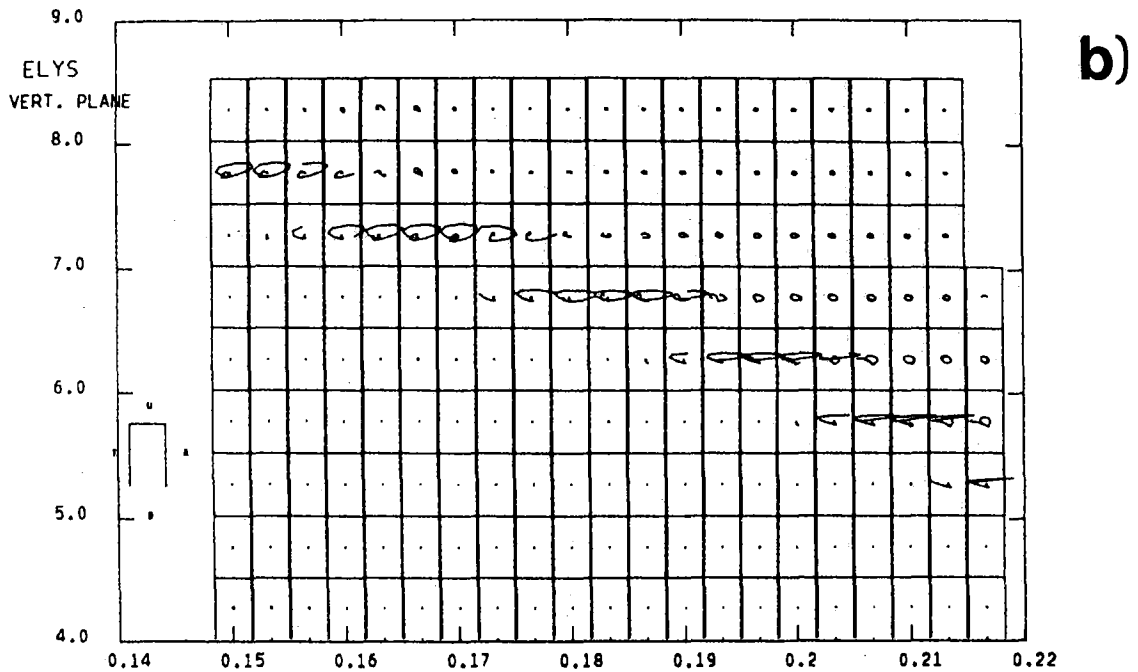
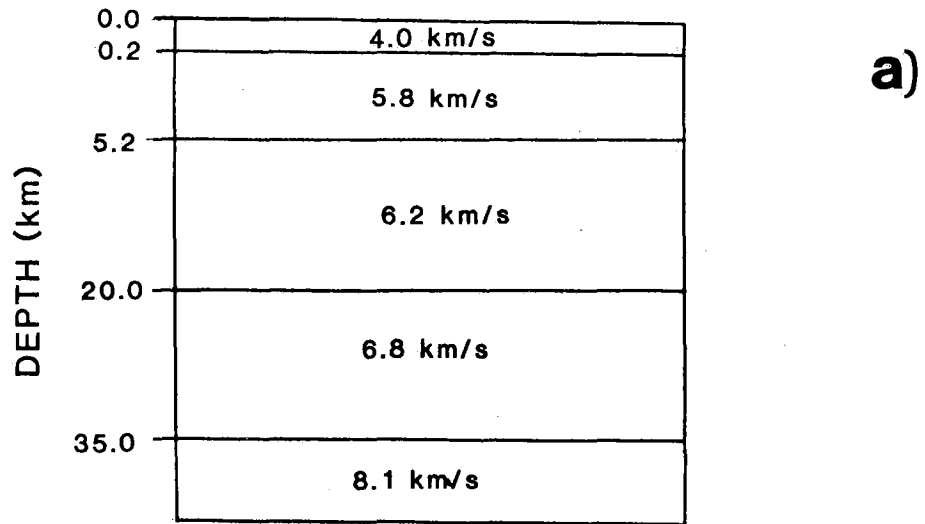


Fig. VII.2.6 a) Crustal model used to generate synthetic S_n .
b) Particle motion in the vertical-radial plane of SV, in response to incident plane SV wave in the model of a).